

## Article

# Impact of the COVID-19 Lockdown on Air Quality Trends in Guiyang, Southwestern China

Zhihua Su <sup>1,\*</sup> , Zongqi Duan <sup>2</sup>, Bing Deng <sup>1</sup>, Yunlong Liu <sup>1</sup> and Xing Chen <sup>1</sup>

<sup>1</sup> School of Management Science, Guizhou University of Finance and Economics, Guiyang 550025, China; 201601137@mail.gufe.edu.cn (B.D.); 201801012@mail.gufe.edu.cn (Y.L.); xingc9804@gmail.com (X.C.)

<sup>2</sup> State Key Laboratory of Resources and Environmental Information System, Institute of Geographic Sciences and Natural Resources Research Chinese Academy of Sciences, Beijing 100101, China; duanzq@igsrr.ac.cn

\* Correspondence: 201201063@mail.gufe.edu.cn

**Abstract:** The absence of motor vehicle traffic and suspended human activities during the COVID-19 lockdown period in China produced a unique experiment to assess the efficiency of air pollution mitigation. Herein, we synthetically analyzed monitoring data of atmospheric pollutants together with meteorological parameters to investigate the impact of human activity pattern changes on air quality in Guiyang, southwestern China. The results show that the Air Quality Index (AQI) during the lockdown period decreased by 7.4% and 23.48% compared to pre-lockdown levels and the identical lunar period during the past 3 years, respectively, which exhibited optimal air quality due to reduced emissions. The sharp decrease in NO<sub>2</sub> concentration reduced the “titration” effect and elevated the O<sub>3</sub> concentration by 31.94% during the lockdown period. Meteorological conditions significantly impacted air quality, and serious pollution events might also occur under emission reductions. Falling wind speeds and increasing relative humidity were the direct causes of the pollution event on February 1st. The “first rain” increases the hygroscopicity of atmospheric particulate matter and then elevate its concentration, while continuous rainfall significantly impacted the removal of atmospheric particulate matter. As impacted by the lockdown, the spatial distribution of the NO<sub>2</sub> concentration sharply decreased on the whole, while the O<sub>3</sub> concentration increased significantly. The implications of this study are as follows: Measures should be formulated to prevent O<sub>3</sub> pollution when emission reduction measures are being adopted to improve air quality, and an emphasis should be placed on the impact of secondary aerosols formation by gas-particle conversion.

**Keywords:** COVID-19; lockdown; air quality; meteorological conditions; Guiyang



**Citation:** Su, Z.; Duan, Z.; Deng, B.; Liu, Y.; Chen, X. Impact of the COVID-19 Lockdown on Air Quality Trends in Guiyang, Southwestern China. *Atmosphere* **2021**, *12*, 422. <https://doi.org/10.3390/atmos12040422>

Academic Editor: Begoña Artíñano

Received: 14 March 2021

Accepted: 23 March 2021

Published: 25 March 2021

**Publisher's Note:** MDPI stays neutral with regard to jurisdictional claims in published maps and institutional affiliations.



**Copyright:** © 2021 by the authors. Licensee MDPI, Basel, Switzerland. This article is an open access article distributed under the terms and conditions of the Creative Commons Attribution (CC BY) license (<https://creativecommons.org/licenses/by/4.0/>).

## 1. Introduction

The outbreak of Coronavirus Disease 2019 (COVID-19) has imposed an unprecedented social impact on China [1]. The State Council of China issued the National Emergency Plan for Public Emergencies to practice social distancing, take compulsory measures to abide by the law to stop all large-scale mass activities (e.g., fairs and rallies), rigorously control traffic, as well as restrict residents from going out for work and classes [2,3]. Hubei, Wuhan announced its lockdown on 23 January 2020, and other major cities/counties in China followed. Localities determine the level of warning [2], i.e., first-level (particularly severe), second-level (serious), third-level (heavier) and fourth-level (general), complying with the degree of harm, urgency and development that COVID-19 may cause. The lockdown in the respective city lasted for at least 3 weeks. During the lockdown period, human activities and their pollutant emissions were significantly restricted, and a “natural laboratory” was built to evaluate the response of air quality to human-made emission reductions [4]. Focus has been placed on the impact exerted by the lockdown of the COVID-19 on air quality in the field of atmospheric environmental research. The research consists of: (1) the range of changes in the concentration of air pollutants that are in account of the reduction in human activities [2]; (2) the temporal and spatial difference in the effect of lockdown on air

quality, and the variation in PM<sub>2.5</sub> chemical composition and the formation of secondary aerosols [4,5]; (3) the change in NO<sub>x</sub> concentrations during a range of lockdown stages [6]; (4) the degree of air quality improvement, as well as the relationship between the urban migration index and alterations in atmospheric pollutant concentrations [7].

Air pollution has sophisticated causes. Besides pollution source emissions, air quality is largely affected by meteorological conditions [8]. The discharge of pollutants materially underpins the occurrence of air pollution events, and meteorological conditions determine the diffusion, transmission, transformation and sedimentation of pollutants [9–12]. Meteorological conditions have a major effect on air quality in the case of relatively stable pollution source emissions [13,14]. Accordingly, it is not necessarily indicated from the reduction in pollution sources that air quality will be improved due to adverse weather conditions. For instance, during the COVID-19 lockdown period, when pollution sources were shut down, severe air pollution events continued to occur in the North China Plain, and emission reductions cannot avoid the occurrence of haze [15]. Existing studies on the impact of the COVID-19 lockdown on China's air quality are largely distributed in the economically developed eastern and central regions. However, relevant research records remain insufficient in the economically underdeveloped western regions. Large-scale cities in the east and central regions of China commonly have large populations, complete industries, as well as various emission sources. However, air pollution sources are mostly motor vehicle emissions in the economically underdeveloped western cities of China, especially tourist cities. As a result, the impact of lockdown on air quality may be inconsistent with that of central and eastern cities in China. Additionally, the existing research records highlighted statistical averages and models to simulate changes of air quality, and actual pollution events have been rarely studied, which hinders the clarification of specific changes in air quality. Thus, in this study, Guiyang, a city in southwest China, was deliberately selected as the research area. The detailed changes of Air Quality Index (AQI) and the mass concentrations of air pollutants PM<sub>2.5</sub>, PM<sub>10</sub>, SO<sub>2</sub>, NO<sub>2</sub>, CO and O<sub>3</sub> before and after the lockdown were compared. Given the meteorological data of the identical period, actual cases were also introduced to determine the impact of the lockdown and variations in meteorological conditions on the air quality in Guiyang. The results have the potential to scientifically underpin air environment management in southwestern China and tourist cities in other regions as well.

## 2. Materials and Methods

### 2.1. Regional Overview and Data Sources

Guiyang, the central part of Guizhou Province, is located on the Yunnan-Guizhou Plateau in southwestern China (26°11'~26°55' N, 106°07'~107°17' E). Guiyang is the capital of Guizhou Province, a national-level big data center, and an essential ecological leisure and tourist city in China. As of November 2020, Guiyang has a permanent population of 4,971,400, an urban population of 3,784,700, as well as an urbanization rate of 76.13%. The China Environmental Monitoring Center has set up 10 national control stations for environmental air monitoring in Guiyang City (Figure 1) to monitor the concentration of air pollutants. The air quality monitoring method was employed by complying with the "Ambient Air Quality Standard" (GB 3095-2012), and the monitoring instruments were regularly calibrated following the "Technical Specification for Automatic Monitoring of Ambient Air Quality" (HJ/T193-2005), in an attempt to ensure the accuracy of the monitored data. The pollutant concentration data monitored by the respective site were published on the Internet in real time (<http://www.aqistudy.cn/> (accessed on 14 February 2020); <http://data.epmap.org/> (accessed on 14 February 2020)). The air quality data selected in the present study included AQI, PM<sub>2.5</sub>, PM<sub>10</sub>, SO<sub>2</sub>, NO<sub>2</sub>, CO and O<sub>3</sub>. Additionally, meteorological observation data over the identical period were selected in this study to determine the impact of meteorological variations on the concentration of atmospheric pollutants, which involved sunshine hours (h), temperature (°C), wind speed (m/s), relative humidity (%) and rainfall (mm). The meteorological observation data originated from Guiyang National

Basic Meteorological Station (WMOID = 57816) (<http://data.cma.cn/user/toLogin.html/> (accessed on 14 February 2020)).

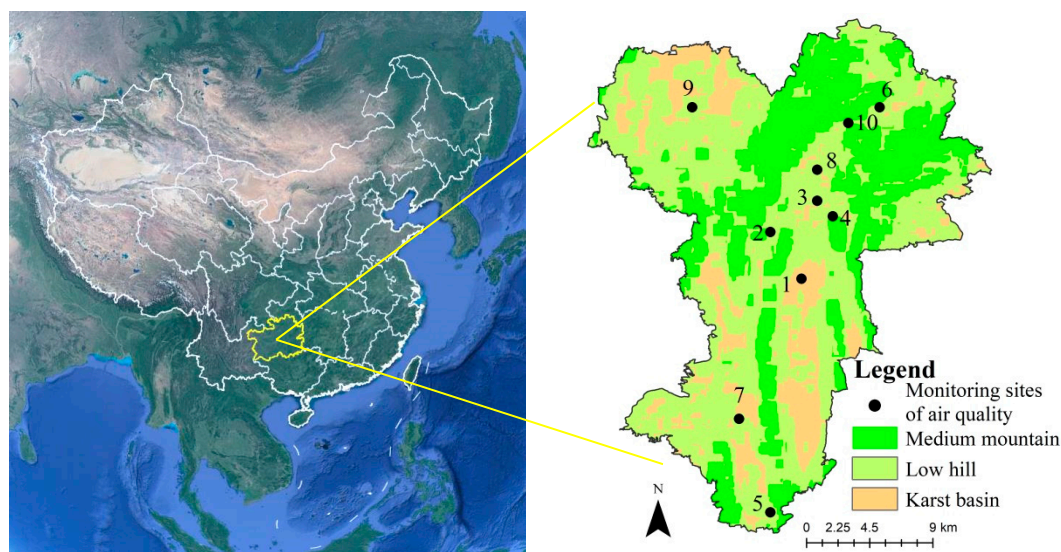


**Figure 1.** Geographical location and landform of Guiyang City and the distribution of air quality stations (based on Google Earth).

## 2.2. Research Methods

On 23 January 2020, Guiyang City issued the “Emergency Notice on the Cancellation of Various Organized Group Activities in the City”. On 24 January 2020, the People’s Government of Guizhou Province decided to roll out the first-level response to public health emergencies. Subsequently, Guiyang’s epidemic prevention measures consisted of closing all cultural and entertainment venues, scenic spots and other public places, rolling out lockdown management in urban communities, limiting each household to appoint one family member to go out for daily necessities purchase every 2 days, and fully achieving fixed-point “contactless” distribution of daily necessities. The lockdown period of this study was selected from 23 January to 13 February 2020 (overall 3 weeks). 1 January to 22 January 2020 (3 weeks on the whole) was the stage of pre-lockdown. Additionally, to compare the average air quality during the 2020 lockdown and the identical lunar period over the past 3 years (2017–2019), the air quality data of the identical lunar period over the last 3 years were selected as the arithmetic average in order to calculate the average air quality and pollutant concentration for the identical lunar period over the past 3 years. The air quality data applied in the present study were all based on hourly concentrations, and the average mass concentration of different time scales (day, lockdown period, pre-lockdown period, and the identical lunar period over the last 3 years) was calculated via using hourly concentrations.

According to the “Technical Regulation on Ambient Air Quality Index (on trial)” (HJ 633—2012), the calculation methods for the ambient air quality index (AQI) are as follows.

$$AQI = \max\{IAQI_1, IAQI_2, IAQI_3, \dots, IAQI_n\} \quad (1)$$

$$IAQI_p = \frac{IAQI_{Hi} - IAQI_{L0}}{BP_{Hi} - BP_{L0}} (C_p - BP_{L0}) + IAQI_{L0} \quad (2)$$

IAQI is the air quality sub-index.  $n$  is the pollutant item.  $IAQI_p$  is the air quality sub-index of the pollutant item  $P$ .  $C_p$  is the mass concentration value of the pollutant item  $P$ .  $BP_{Hi}$  is the pollutant concentration limit close to  $C_p$ .  $BP_{L0}$  is the low value of the pollutant concentration limit close to  $C_p$ ,  $IAQI_{Hi}$  is the air quality index corresponding to  $BP_{Hi}$ .  $IAQI_{L0}$  is the air quality index corresponding to  $BP_{L0}$ .

Interpolation is commonly used to study the spatial distribution of pollutant concentrations. It calculates the data of other unknown points in the identical area through the value of known points to yield the spatial distribution of pollutant concentration of the entire area. Inverse Distance Weighted Interpolation (IDW) complies with the principle of similarity and weighted average with the distance between the interpolation point and the sample point [16]. It is assumed that a series of discrete points are distributed on a plane, and their coordinates and values are known as  $X_i, Y_i, Z_i$  ( $i = 1, 2, \dots, n$ ). According to the value of the surrounding discrete points, the value of  $Z$  point is obtained by the distance weighted value, formulas are as follows.

$$z = \left[ \sum_i^n \frac{z_i}{d_i^2} \right] / \left[ \sum_i^n \frac{1}{d_i^2} \right] \quad (3)$$

$$d_i^2 = (X - X_i)^2 + (Y - Y_i)^2 \quad (4)$$

ArcGIS 10.2 software was used in this study, and IDW was selected for interpolation to explore the spatial distribution characteristics of the pollutants ( $\text{NO}_2$  and  $\text{O}_3$ ) that have changed significantly before and after the lockdown in Guiyang, as well as analyze their factors.

### 3. Results

#### 3.1. Comparison of Air Quality in Different Periods

Figure 2 shows that the AQI during the lockdown period in 2020 decreased by 3.14 (7.4%) and 12.11 (23.48%) as compared with that of the pre-lockdown period and the identical lunar period during the past 3 years, respectively, which exhibited the optimal air quality due to reduced emissions. The average concentrations of  $\text{PM}_{10}$ ,  $\text{PM}_{2.5}$ ,  $\text{NO}_2$  and CO during the lockdown period declined by 16.45%, 6.23%, 49.88% and 18.18%, respectively, compared with the pre-lockdown period, and decreased by 31.19%, 26.54%, 50.12% and 16.7%, respectively, in comparison with the identical lunar period during the past 3 years. The  $\text{NO}_2$  concentration, in particular, dropped sharply during the lockdown period, which was nearly half of that the pre-lockdown period and the identical lunar period during the past 3 years. However, the average concentrations of  $\text{SO}_2$  and  $\text{O}_3$  both increased during the lockdown period, and  $\text{SO}_2$  increased slightly by 4.6% ( $0.64 \mu\text{g}\cdot\text{m}^{-3}$ ). The average  $\text{O}_3$  concentration rose sharply, from  $45.68 \mu\text{g}\cdot\text{m}^{-3}$  during the pre-lockdown period, to  $60.27 \mu\text{g}\cdot\text{m}^{-3}$  during the lockdown period, marking an increase of 31.94%. The  $\text{SO}_2$  concentration increased slightly during the lockdown period since Chinese industrial and residential sectors have implemented strong emission reduction measures over the past few years, which have already greatly decreased  $\text{SO}_2$  concentration in the environment [17]. As a result, the COVID-19 Lockdown could not reduce the  $\text{SO}_2$  concentration. The largest source of  $\text{NO}_x$  emissions originated from transportation sources [18]. The sharp drop in  $\text{NO}_2$  concentration was related to the sharp drop in motor vehicle activity that was attributed to lockdown. Moreover, the reduction in motor vehicles led to a decline in NO emissions. Thus, the consumption of  $\text{O}_3$  was reduced by “titration” [19]. Additionally, the  $\text{O}_3$  concentration increased noticeably during the epidemic period.

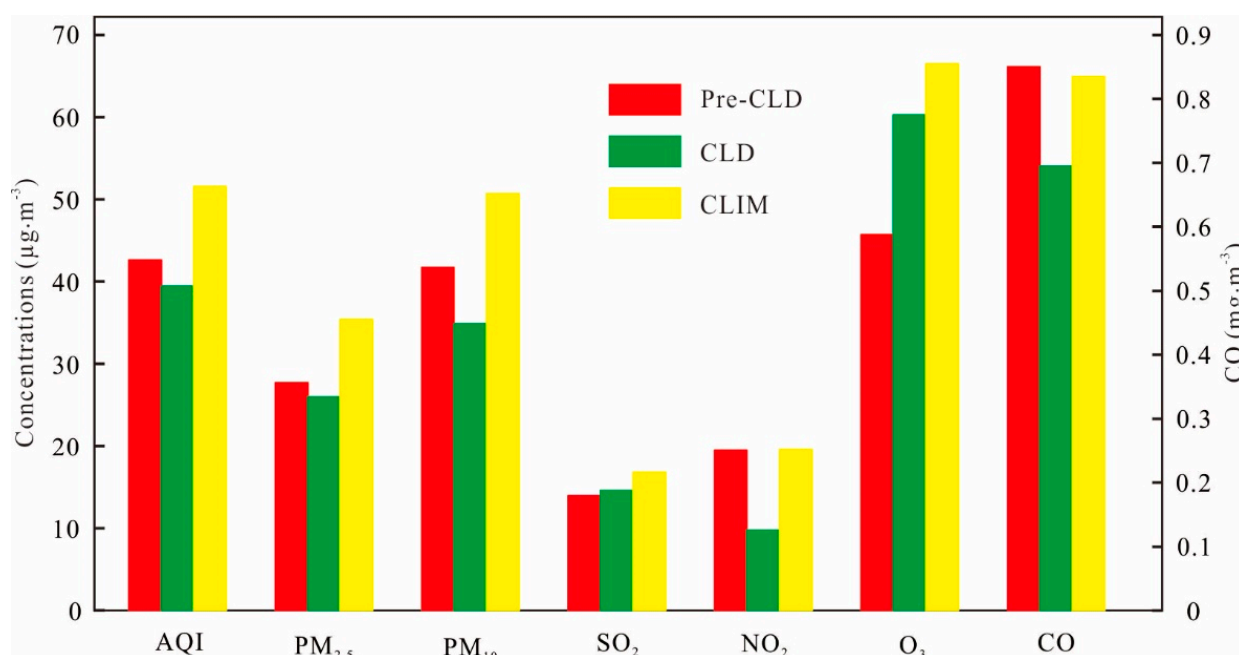


**Figure 2.** Average air quality during the pre-lockdown, lockdown, and the identical lunar period during the past 3 years (CLD: Three week COVID19 lockdown period from 23 January to 13 February 2020; pre-CLD: Three weeks before CLD for from 1 January to 22 January 2020; CLIM: 2017–2019 year, the same as that in 2020-CLD in the Chinese lunar calendar).

### 3.2. Daily Changes in Air Quality before and after Lockdown

Figure 3 indicates that the air quality before and after lockdown was significantly different. The overall AQI before lockdown was higher than that during lockdown, suggesting more severe pollution. During the lockdown period, except for a serious pollution event on 1 February, the AQI for the rest of the period was generally low, and the air quality was good; moreover, the daily average concentrations of PM<sub>10</sub>, PM<sub>2.5</sub>, NO<sub>2</sub> and CO were overall lower, except for those on 1 February. The daily average concentration of NO<sub>2</sub> decreased the most during the lockdown period, and the response to the reduction in vehicle emissions was the most significant. On 30 January 2020, there was an obvious pollution event in SO<sub>2</sub>, while the concentration of other pollutants did not increase significantly. This revealed the different sources of SO<sub>2</sub> pollution. The peak and valley values of O<sub>3</sub> concentration did not effectively correspond to PM<sub>2.5</sub>, PM<sub>10</sub>, SO<sub>2</sub>, NO<sub>2</sub> and CO, suggesting that O<sub>3</sub>, i.e., a secondary pollutant, was also affected by the concentrations of precursors and the formation of photochemical reactions [19]. NO<sub>2</sub> acted as a key component of atmospheric chemical processes and a crucial precursor for the formation of O<sub>3</sub> and secondary aerosol [20]. During the lockdown period, under the significant drop in NO<sub>x</sub> concentrations, the “titration” effect (O<sub>3</sub>+NO→NO<sub>2</sub>+O<sub>2</sub>) was reduced, so the daily average O<sub>3</sub> concentration increased on the whole [4,19].

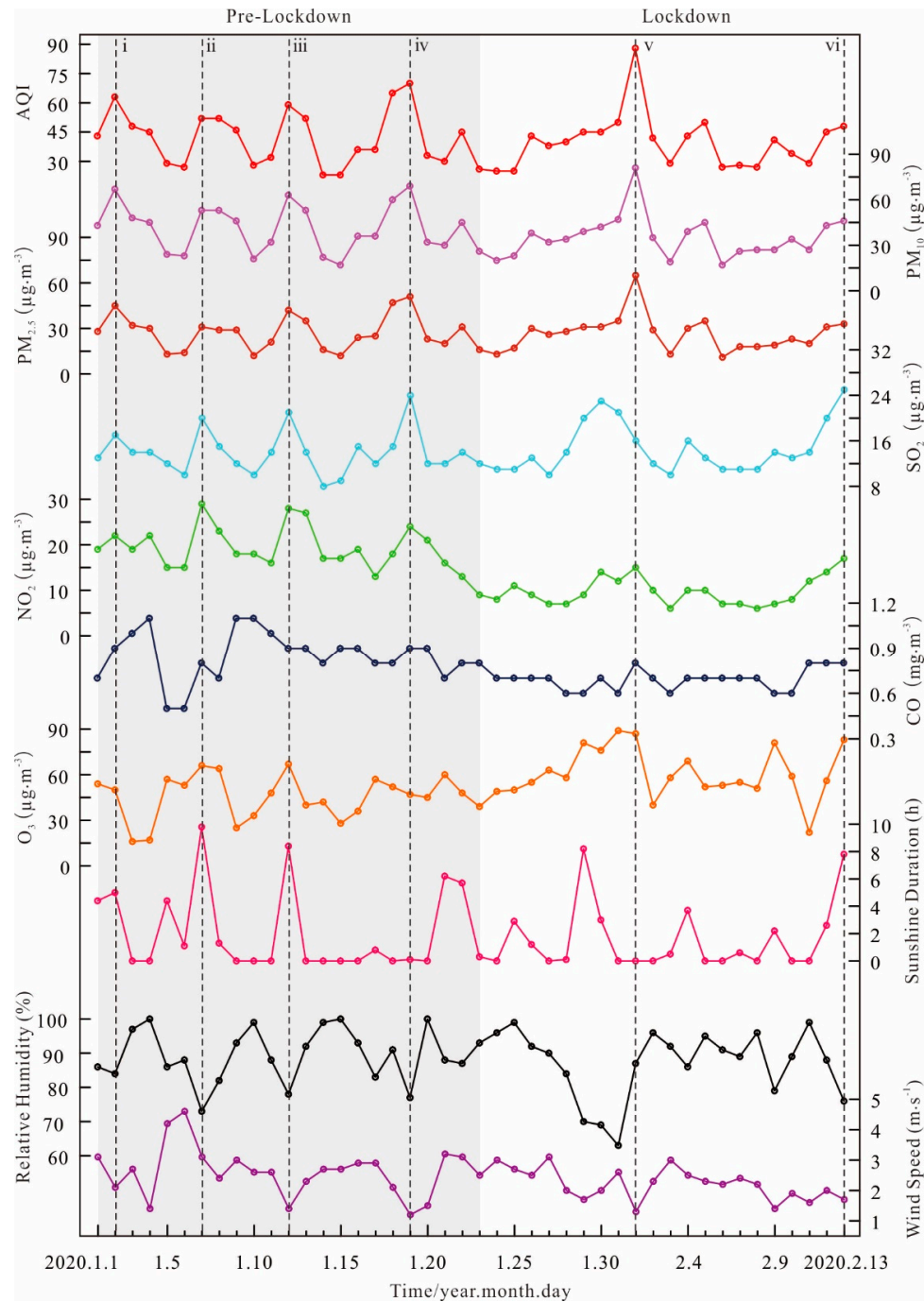


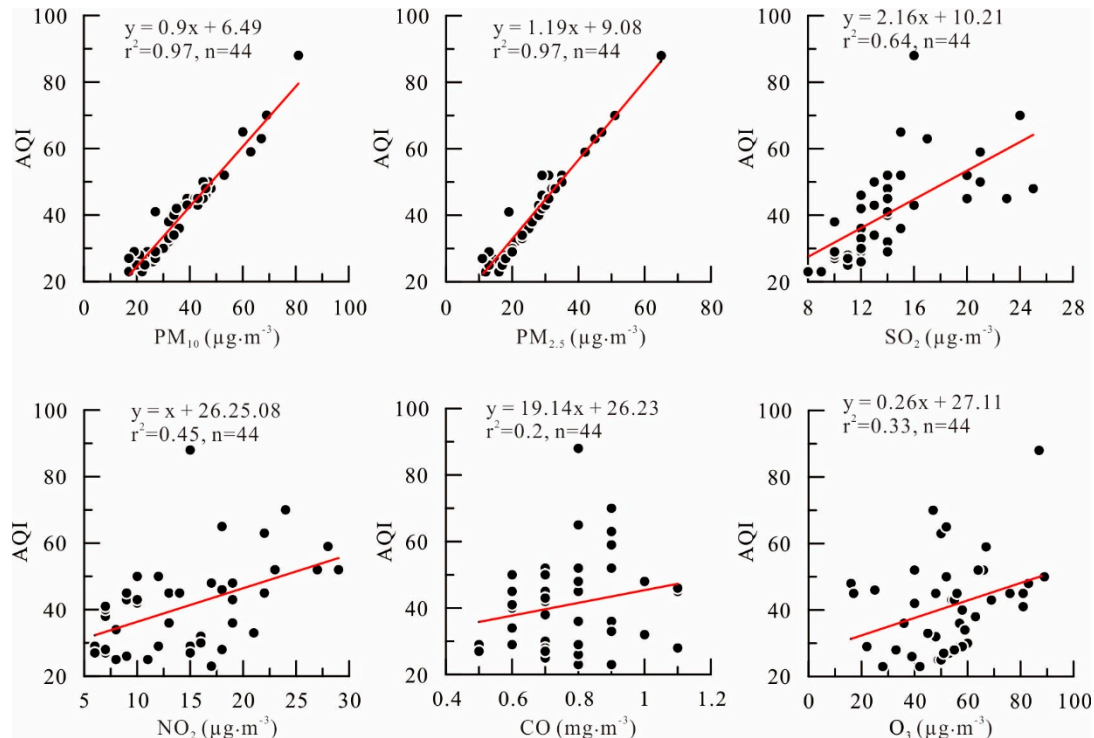
**Figure 3.** Daily variations of air quality during pre-lockdown and lockdown in 2020.

Variations in meteorological conditions had a vital impact on changes in the concentrations of pollutants, leading to large fluctuations in the concentrations of pollutants before and after lockdown, over a short period of time. In most cases, the peaks of PM<sub>2.5</sub>, PM<sub>10</sub>, SO<sub>2</sub>, and NO<sub>2</sub> concentrations correspond to the peaks of sunshine hours (Figure 3i–vi), relative humidity valley values (Figure 3i–iv,vi), and wind speed valley values (Figure 3i,iii–vi), respectively. Due to the long sunshine hours, the temperature rose, and evaporation increased, thereby resulting in a decrease in the relative humidity and a dry surface. Accordingly, pollutants on the ground, especially dust, were more likely to fly into the air. Meantime, there was little wind, resulting in the pollution sources not being easily spread and gradually accumulating, leading to an increase in the concentration. On 11 February, the relative humidity was high, and the sunshine hours were the lowest;

which is not conducive for the occurrence of photochemical reactions. As a result, the daily average concentration of  $O_3$  was abnormally low. Influenced by adverse weather conditions, a severe air pollution incident occurred on 1 February during the lockdown period (see Section 3.3 for a detailed analysis).

The peak value of the  $O_3$  concentration corresponded to that of sunshine hours, relative humidity and wind speed (Figure 3). It was suggested that the greater the number of sunshine hours and the lower the relative humidity, the more significant the photochemical reaction will be in terms of synthesizing  $O_3$ . Under calm wind conditions,  $O_3$  accumulated. Although there were few sunshine hours and weak solar radiation in winter, the  $O_3$  concentration significantly increased on sunny days with a greater number of sunshine hours (Figure 3). It was, therefore, indicated that photochemical reaction remains essential for  $O_3$  synthesis although solar radiation is weak in winter. Meteorological conditions varied significantly, and the photochemical reactions in different periods show various strengths, which caused the  $O_3$  concentration to fluctuate more significantly.

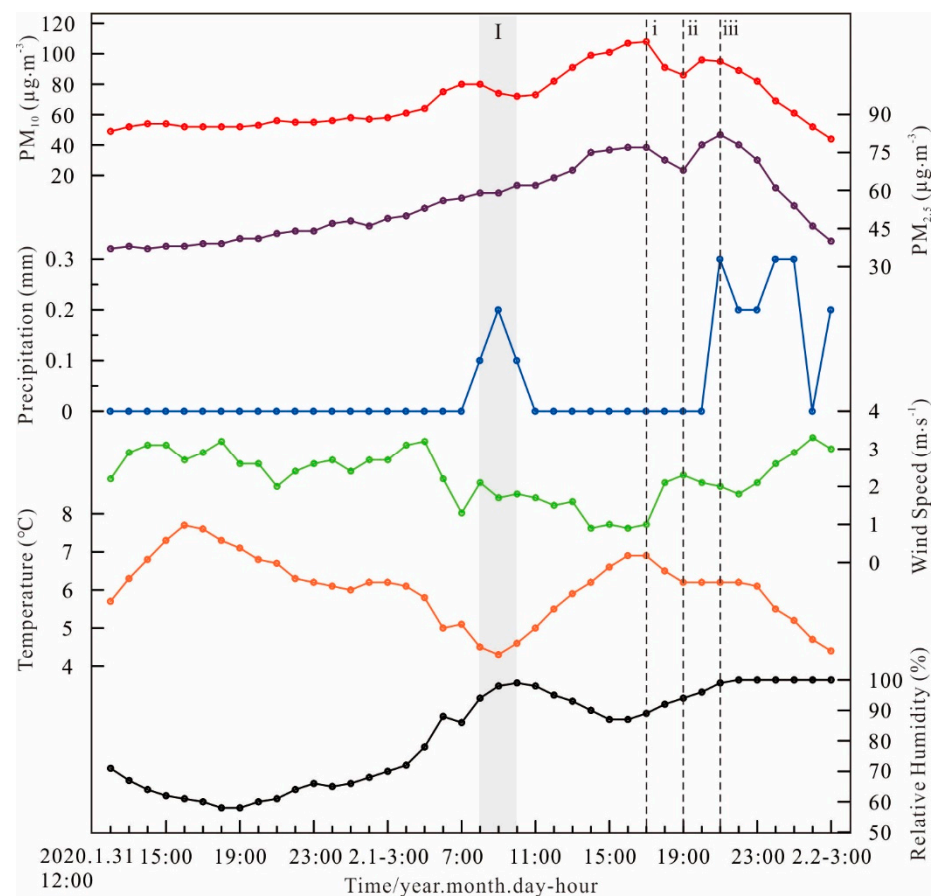
According to Figure 3,  $PM_{10}$  and  $PM_{2.5}$  exhibited peak-to-peak and valley-to-valley synchronous fluctuations with the AQI, whether before or after lockdown. The other pollutants (i.e.,  $SO_2$ ,  $NO_2$ ,  $CO$ , and  $O_3$ ) showed more variable trends with the AQI, which indicated that particulate matter  $PM_{10}$  and  $PM_{2.5}$  were the main pollutants influencing air quality changes. The correlation coefficients of AQI and  $PM_{2.5}$ ,  $PM_{10}$ ,  $SO_2$ ,  $NO_2$ ,  $CO$  and  $O_3$  were 0.97, 0.97, 0.64, 0.2, 0.45, and 0.33, respectively (Figure 4). The AQI achieved the largest correlation coefficient with  $PM_{2.5}$  and  $PM_{10}$ , a certain degree of correlation with  $SO_2$  and  $NO_2$ , in addition to the smallest correlation coefficient with  $CO$  and  $O_3$ . The magnitude of the correlation coefficient confirmed that  $PM_{10}$  and  $PM_{2.5}$  were the primary pollutants dominating changes in air quality, followed by  $SO_2$  and  $NO_2$ , and then  $CO$  and  $O_3$ .



**Figure 4.** The correlation between Air Quality Index (AQI) and the daily average concentrations of  $PM_{10}$ ,  $PM_{2.5}$ ,  $SO_2$ ,  $NO_2$ ,  $CO$ , and  $O_3$ .

### 3.3. Case Analysis of Heavy Pollution

On 1 February 2020, the AQI reached 88, which was the maximum value during the lockdown period and significantly higher than any peak value during the pre-lockdown period. The most severe pollution event also occurred under the conditions of emission reductions during the lockdown period. Since  $PM_{10}$  and  $PM_{2.5}$  were the primary pollutants affecting air quality, we chose the hourly average concentrations of  $PM_{2.5}$  and  $PM_{10}$  from 12:00 on 31 January to 3:00 on 2 February 2020 and the meteorological parameters of the identical period. The time series analysis method was employed to study the pollution event in detail. Figure 5 suggests that from 12:00 on 31 January 2020 to 16:00 on 1 February, the wind speed ceaselessly fluctuated and decreased to 0.9 m/s, the temperature decreased, and the relative humidity increased. There was no rain during the entire period from 8:00 to 10:00 on 1 February. The decrease in temperature and wind speed and the increase in humidity caused the accumulation of particulate matter in the air.  $PM_{10}$  and  $PM_{2.5}$  reached peaks of 108 and  $77 \mu\text{g}\cdot\text{m}^{-3}$  at 17:00 on 1 February, respectively (Figure 5i). Then, the wind speed increased slowly, reaching 2.3 m/s at 19:00 on 1 February. The increase in wind speed caused the particulate matter to diffuse to a certain extent, reducing the concentrations of  $PM_{10}$  and  $PM_{2.5}$  to 86 and  $68 \mu\text{g}\cdot\text{m}^{-3}$ , respectively (Figure 5ii). When the precipitation reached 0.3 mm at 21:00 on February 1st, the moisture absorption of particulate matter increased and the wind speed decreased; the dual effect caused the particle concentration to increase again (Figure 5iii). Since then, as the rainfall continued, the “wet deposition” of particulate matter increased, and the wind speed was elevated, thereby facilitating the diffusion of particulate matter. The concentrations of  $PM_{10}$  and  $PM_{2.5}$  declined to 44 and  $40 \mu\text{g}\cdot\text{m}^{-3}$  at 3:00 on 2 February, indicating the end of the pollution event.



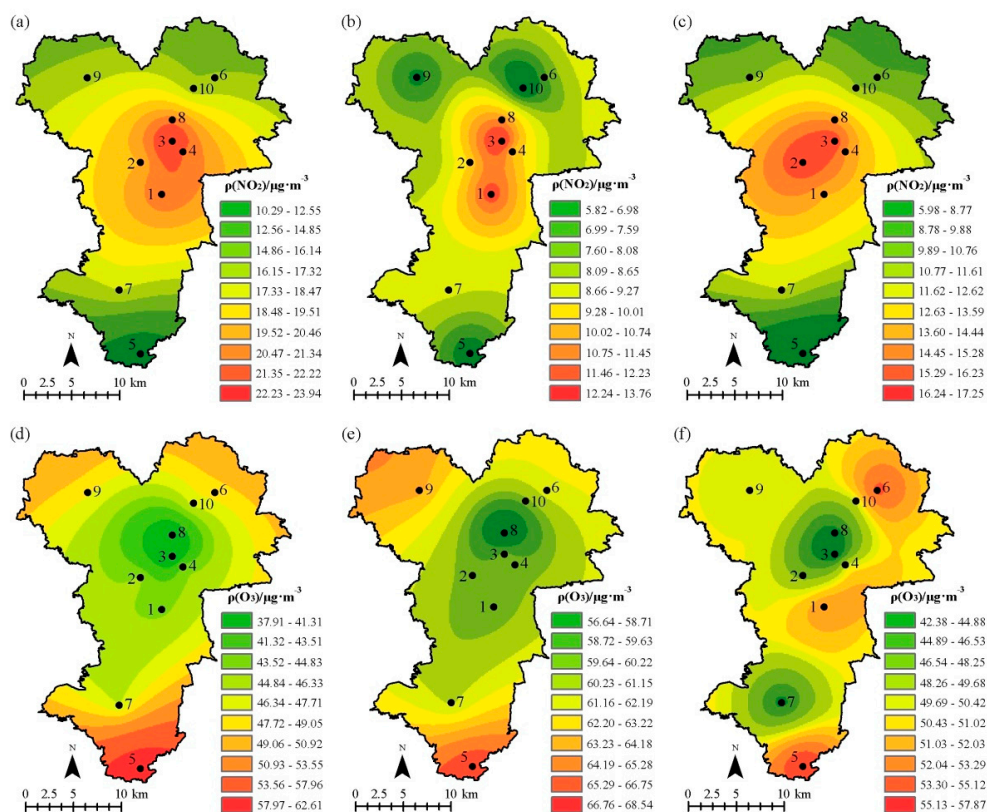
**Figure 5.** Variations of  $PM_{10}$ ,  $PM_{2.5}$  concentration, and meteorological parameters from 12:00 on 31 January 2020 to 3:00 on 2 February 2020.

Figure 5 shows that from 12:00 on 31 January 2020 to 17:00 on 1 February, the concentration of  $PM_{10}$  and  $PM_{2.5}$  gradually increased in the fluctuating process, while the temperature first decreased and then increased, and the relative humidity first increased and then decreased. It can be seen that the influence of temperature and relative humidity on the concentration of  $PM_{10}$  and  $PM_{2.5}$  was more complicated, and the relationship between the two and the concentration of particulate matter was non-linear. High levels of precipitation, reaching 0.3 mm, occurred at 21:00 on 1 February. As suggested from the rebound of  $PM_{10}$  and  $PM_{2.5}$  concentrations, rainfall positively impacted the concentration of particulate matter. In other words, rainfall caused atmospheric particles to absorb moisture, elevating their concentration. However, as the rainfall continued, the concentrations of  $PM_{10}$  and  $PM_{2.5}$  declined rapidly, suggesting the “wet deposition” removal effect of rainfall [21]. To a certain extent, the rainfall that occurred from 8:00 to 10:00 on 1 February decreased  $PM_{10}$  concentration, whereas it hardly affected the  $PM_{2.5}$  concentration (Figure 5I). It is, therefore, suggested that the “wet deposition” effect of rainfall on the coarse particulate matter  $PM_{10}$  was more significant than that of the fine particulate matter  $PM_{2.5}$ . Since  $PM_{10}$  exhibits a larger particle size than  $PM_{2.5}$ , it is more easily combined with rainwater in the air and it then settles under the action of gravity, thereby leading to the observed decrease in its concentration. In summary, the impact of precipitation on the concentration of particulate matter was more complicated. “First rain” was capable of aggravating atmospheric particulate matter pollution, while continuous rainfall significantly removed atmospheric particulate matter, and precipitation more noticeably removed coarse particles of  $PM_{10}$ .

### 3.4. Spatial Distribution of $NO_2$ and $O_3$

The average concentration of  $NO_2$  and  $O_3$ , with the largest changes in concentration during the lockdown period, were selected to study their spatial distribution characteristics. Figure 6 illustrates that the distribution characteristics of  $NO_2$  and  $O_3$  during the pre-lockdown, lockdown periods and the identical lunar period of the past 3 years were relatively consistent. The average concentration of  $NO_2$  over the three stages was high in the downtown and low in the suburbs, gradually decreasing from the central urban area to the suburbs. The average concentration of  $NO_2$  in Tongmuling, a suburban station, reached the minimum value. As indicated from the spatial distribution characteristics of  $NO_2$  concentration, its concentration changes were mainly affected by vehicle emissions [18]. The level of motor vehicle activity in the downtown was relatively high, and the high emission of nitrogen oxides led to high  $NO_2$  concentrations. The opposite was true in the suburbs. As observed during the lockdown period, the average concentration of  $NO_2$  was low throughout the study area. This demonstrated that the policy of lockdown reduced the activity level of motor vehicles in the entire space, thereby enabling the average concentration of  $NO_2$  in the entire area to drop significantly.

The spatial distribution of  $O_3$  was the opposite to that of  $NO_2$ . The  $O_3$  concentration reached the minimum value in the downtown and the maximum value in the suburbs during the three stages, marking a gradual increase from the center to the periphery. As impacted by human-made emission factors (e.g., motor vehicles), the  $NO$  concentration in urban areas was relatively high. The high concentration of  $NO$  hindered the production of  $O_3$  and “titrated” surface  $O_3$  [19,22]. The suburban vegetation coverage rate was high, and the volatile organic compounds (VOCs) from natural source promoted the production of  $O_3$ , making its concentration higher [23,24]. The  $O_3$  concentration in Tongmuling, a suburban station, reached the highest value, further confirming that VOCs were the primary control factor for  $O_3$  pollution. The average  $O_3$  concentration was higher throughout the space during the lockdown period. This also demonstrated that lockdown reduced the activity level of motor vehicles, thereby leading to the reduction in  $NO$  concentrations in the atmosphere, and the “titration” effect of  $O_3$  was weakened, which led to its accumulated concentration [4,19].



**Figure 6.** Spatial distribution of NO<sub>2</sub> and O<sub>3</sub> concentrations in urban Guiyang during the pre-lockdown, lockdown, and the identical lunar period over the last 3 years (a,d): Pre-lockdown; (b,e): Lockdown; (c,f): The identical lunar period during the past 3 years.

#### 4. Discussion

##### 4.1. Influence of Secondary Aerosols Generated by Gas-Particle Conversion on Pollution

In the atmospheric environment affected by human activities, SO<sub>2</sub> and NO<sub>x</sub> can be oxidized via various chemical pathways to synthesize sulfate and nitrate, respectively. The secondary inorganic compounds in particulates are often sulfates and nitrates [20,25,26]. As highlighted by previously conducted studies, the secondary aerosol formation of sulfate and nitrate is the primary driving factor for the explosive growth of PM<sub>2.5</sub> [27]. During the lockdown period in Guiyang City, the average concentration of NO<sub>2</sub> dropped sharply, the average concentrations of SO<sub>2</sub> and PM<sub>2.5</sub> rose slightly, and the average concentration of O<sub>3</sub> surged (Figure 2). The different trends in the concentrations of air pollutants indicated that the drop in pollution levels during the lockdown period cannot be fully explained by the initial emissions; hence, secondary aerosol production via gas-particle conversion also critically impacted pollution levels [5]. Decreases in the NO<sub>2</sub> concentration would have affected the formation of nitrate aerosols, thereby reducing the PM<sub>2.5</sub> concentration [5]. During the lockdown period in Guiyang City, the PM<sub>2.5</sub> concentration only dropped by 6.23% (Figure 2), which is not consistent with the sharp drop in the NO<sub>2</sub> concentration. This may be explained by SO<sub>2</sub> reacting with OH radicals during the lockdown period, leading to the synthesis of more sulfate aerosols [28], which replaced nitrate aerosols. As a result, PM<sub>2.5</sub> did not decrease significantly. During the lockdown period, PM<sub>10</sub> decreased by 16.45%, which was larger than PM<sub>2.5</sub>, indicating that the secondary aerosols produced largely consisted of PM<sub>2.5</sub>.

##### 4.2. The Impact of Adverse Weather Conditions on Air Quality

On 1 February, the AQI reached the maximum value of 88 during the lockdown period, significantly higher than any peak value during pre-lockdown period. A relatively severe pollution event occurred with the emission reduction background (Figure 3). This

indicates that lockdown cannot completely prevent the occurrence of pollution incidents, which complies with the research records of the North China Plain [15]. According to Figure 5, the continuous decrease in wind speed and the gradual increase in relative humidity were recognized as the meteorological causes of the pollution event on 1 February. The gradual decrease in wind speed resulted in a stagnant state within the atmosphere, making it difficult for pollutants to spread. Consequently, the increase in relative humidity contributed to the formation of secondary aerosols of various gas precursors via gas-phase oxidation and heterogeneous reactions [27]. When the atmosphere was in this stagnant state, the rapid conversion of major gaseous pollutants to secondary aerosols will have been an essential factor facilitating the explosive growth of PM<sub>2.5</sub> [29]. However, as indicated from the “Ambient Air Quality Index (AQI) Technical Regulations (Trial)” (HJ 633~2012), the AQI of Guiyang City on 1 February was 88, which represents good air quality. This may be explained by the fact that Guiyang is located on the Yunnan-Guizhou Plateau, with good ecological conditions, underdeveloped industries, as well as low pollutant emissions.

#### 4.3. Implications for Air Quality Control

Due to the non-linear chemical process and the decreasing “titration” [19], the O<sub>3</sub> concentration during the lockdown period was elevated significantly [4]. This lockdown period was in the winter season with low sunshine hours (Figure 3), hindering the formation of O<sub>3</sub> via the photochemical reaction. Thus, the concentration of O<sub>3</sub> in the atmosphere was relatively low. However, if this lockdown occurred in summer, when photochemical reactions are strong, the O<sub>3</sub> pollution level would inevitably increase significantly. Accordingly, a plan should be formulated to prevent O<sub>3</sub> pollution when adopting emission reduction measures to improve air quality. Additionally, more sulfate aerosols were generated during the lockdown period, which remedied the sharp drop in nitrate aerosols [5], thereby resulting in the PM<sub>2.5</sub> concentration dropping slightly. Thus, environmental management departments should consider the impact of secondary aerosols, generated by gas-particle conversion, on air quality when environmental protection measures are being formulated.

#### 4.4. Limitations

As impacted by the lack of actual sampling and experiments, the actual variations in the chemical composition of PM<sub>2.5</sub> before and after lockdown could not be analyzed, so insufficient insights were gained into the secondary aerosols produced by gas-particle conversion and the mechanisms behind this process. This will be researched in the future.

### 5. Conclusions

The Air Quality Index (AQI) during the lockdown period decreased by 7.4% and 23.48% compared to the pre-lockdown and identical lunar period during the past 3 years, respectively. The average concentrations of PM<sub>10</sub>, PM<sub>2.5</sub>, NO<sub>2</sub>, and CO during the lockdown period decreased by 16.45%, 6.23%, 49.88% and 18.18%, respectively, compared with the pre-lockdown period, and dropped by 31.19%, 26.54%, 50.12% and 16.7%, respectively, compared with the identical lunar period during the past 3 years. The average concentrations of SO<sub>2</sub> and O<sub>3</sub> both increased during the lockdown period. The average concentration SO<sub>2</sub> increased slightly by 4.6%, and the O<sub>3</sub> concentration increased significantly by 31.94%. The sharp decrease in the NO<sub>2</sub> concentration during the epidemic displayed an association with the sharp decrease in motor vehicle activity resulting from the lockdown. The reduction in motor vehicle use led to a decrease in the NO concentration in the atmosphere, and a reduction in the “titration” effect, primarily causing the O<sub>3</sub> concentration to increase substantially during the lockdown period. Atmospheric particulate matter PM<sub>10</sub> and PM<sub>2.5</sub> were suggested as the main pollutants influencing air quality changes, followed by SO<sub>2</sub> and NO<sub>2</sub>, and then CO and O<sub>3</sub>. Additionally, meteorological conditions significantly impacted air quality, and emission reduction cannot avoid pollution events. Temperature and relative humidity had a non-linear relationship with the concentration of atmospheric particles. The impact of precipitation on PM<sub>2.5</sub> and PM<sub>10</sub> was more complicated. “First

rain" increases the moisture absorption of atmospheric particles and their concentration, while continuous rainfall noticeably removed atmospheric particles. Furthermore, the lockdown caused the NO<sub>2</sub> concentration to decrease sharply in spatial distribution and the O<sub>3</sub> concentration to increase significantly.

**Author Contributions:** Investigation, Y.L.; methodology, B.D.; supervision, Z.D.; writing—original draft, X.C.; writing—review and editing, Z.S. All authors have read and agreed to the published version of the manuscript.

**Funding:** This work was supported by the National Natural Science Foundation of China (No.41964005) and the Innovative exploration and new academic seedling project of Guizhou University of Finance and Economics (No.2020XSXMA04).

**Institutional Review Board Statement:** Not applicable.

**Informed Consent Statement:** Not applicable.

**Data Availability Statement:** Data are contained within the article.

**Conflicts of Interest:** The authors declare no conflict of interest. The funders had no role in the design of the study; in the collection, analyses, or interpretation of data; in the writing of the manuscript, or in the decision to publish the results.

## References

1. Bibek, R.; Naveen, P.; Bikal, S.; Moon, T. Air Medical Evacuation of Nepalese Citizen during Epidemic of COVID-19 from Wuhan to Nepal. *J. Nepal Med. Assoc.* **2020**, *58*, 125–133.
2. Li, L.; Li, Q.; Huang, L.; Wang, Q.; Zhu, A.; Xu, J.; Liu, Z.; Li, H.; Shi, L.; Li, R.; et al. Air quality changes during the COVID-19 lockdown over the Yangtze River Delta Region: An insight into the impact of human activity pattern changes on air pollution variation. *Sci. Total Environ.* **2020**, *732*, 139–282. [[CrossRef](#)] [[PubMed](#)]
3. Tian, H.; Liu, Y.; Li, Y.; Wu, C.-H.; Chen, B.; Kraemer, M.; Li, B.; Cai, J.; Xu, B.; Yang, Q.; et al. An investigation of transmission control measures during the first 50 days of the COVID-19 epidemic in China. *Science* **2020**, *368*, 638–642. [[CrossRef](#)]
4. Le, T.; Wang, Y.; Liu, L.; Yang, J.; Yung, Y.L.; Li, G.; Seinfeld, J.H. Unexpected air pollution with marked emission reductions during the COVID-19 outbreak in China. *Science* **2020**, *369*, 702–706. [[CrossRef](#)] [[PubMed](#)]
5. Chen, H.; Huo, J.; Fu, Q.; Duan, Y.; Xiao, H.; Chen, J. Impact of quarantine measures on chemical compositions of PM<sub>2.5</sub> during the COVID-19 epidemic in Shanghai, China. *Sci. Total Environ.* **2020**, *743*, 140758. [[CrossRef](#)] [[PubMed](#)]
6. Zhang, R.; Zhang, Y.; Lin, H.; Feng, X.; Fu, T.-M.; Wang, Y. NO<sub>x</sub> Emission Reduction and Recovery during COVID-19 in East China. *Atmosphere* **2020**, *11*, 433. [[CrossRef](#)]
7. Bao, R.; Zhang, A. Does lockdown reduce air pollution? Evidence from 44 cities in northern China. *Sci. Total Environ.* **2020**, *731*, 139052. [[CrossRef](#)] [[PubMed](#)]
8. Shi, C.; Yuan, R.; Wu, B.; Meng, Y.; Zhang, H.; Zhang, H.; Gong, Z. Meteorological conditions conducive to PM<sub>2.5</sub> pollution in winter 2016/2017 in the Western Yangtze River Delta, China. *Sci. Total Environ.* **2018**, *642*, 1221–1232. [[CrossRef](#)] [[PubMed](#)]
9. Cai, Z.; Jiang, F.; Chen, J.; Jiang, Z.; Wang, X. Weather Condition Dominates Regional PM<sub>2.5</sub> Pollutions in the Eastern Coastal Provinces of China during Winter. *Aerosol Air Qual. Res.* **2018**, *18*, 969–980. [[CrossRef](#)]
10. Gui, K.; Che, H.; Wang, Y.; Wang, H.; Zhang, L.; Zhao, H.; Zheng, Y.; Sun, T.; Zhang, X. Satellite-derived PM<sub>2.5</sub> concentration trends over Eastern China from 1998 to 2016: Relationships to emissions and meteorological parameters. *Environ. Pollut.* **2019**, *247*, 1125–1133. [[CrossRef](#)]
11. Li, X.; Ma, Y.; Wang, Y.; Liu, N.; Hong, Y. Temporal and spatial analyses of particulate matter (PM<sub>10</sub> and PM<sub>2.5</sub>) and its relationship with meteorological parameters over an urban city in northeast China. *Atmos. Res.* **2017**, *198*, 185–193. [[CrossRef](#)]
12. Wang, P.; Guo, H.; Hu, J.; Kota, S.H.; Ying, Q.; Zhang, H. Responses of PM<sub>2.5</sub> and O<sub>3</sub> concentrations to changes of meteorology and emissions in China. *Sci. Total Environ.* **2019**, *662*, 297–306. [[CrossRef](#)] [[PubMed](#)]
13. Pateraki, S.; Asimakopoulos, D.N.; Flocas, H.A.; Maggos, T.; Vasilakos, C. The role of meteorology on different sized aerosol fractions (PM<sub>10</sub>, PM<sub>2.5</sub>, PM<sub>2.5–10</sub>). *Sci. Total Environ.* **2012**, *419*, 124–135. [[CrossRef](#)]
14. Tai, A.P.K.; Mickley, L.J.; Jacob, D.J. Correlations between fine particulate matter (PM<sub>2.5</sub>) and meteorological variables in the United States: Implications for the sensitivity of PM<sub>2.5</sub> to climate change. *Atmos. Environ.* **2010**, *44*, 3976–3984. [[CrossRef](#)]
15. Wang, P.; Chen, K.; Zhu, S.; Wang, P.; Zhang, H. Severe air pollution events not avoided by reduced anthropogenic activities during COVID-19 outbreak. *Resour. Conserv. Recycl.* **2020**, *158*, 104814. [[CrossRef](#)] [[PubMed](#)]
16. Dong, Z.; Zheng, S.; Zhao, H.; Dong, R. Comparative analysis of methods of wind field simulation based on spatial interpolation. *J. Geo-Inf. Sci.* **2015**, *17*, 37–44. (In Chinese)
17. Zhang, Q.; Zheng, Y.; Tong, D.; Shao, M.; Wang, S.; Zhang, Y.; Xu, X.; Wang, J.; He, H.; Liu, W.; et al. Drivers of improved PM<sub>2.5</sub> air quality in China from 2013 to 2017. *Proc. Natl. Acad. Sci. USA* **2019**, *116*, 24463–24469. [[CrossRef](#)] [[PubMed](#)]

18. Zhang, M.; Chen, W.; Gao, C.; Zhang, X.; Jiang, Y.; Xiu, A. Spatio-temporality of anthropogenic air pollutants in Northeast China based on current emission inventories. *Sci. Geogr. Sin.* **2020**, *40*, 1940–1948. (In Chinese)
19. Wang, Z.; Li, Y.; Chen, T.; Zhang, D.; Sun, F.; Wei, Q.; Dong, X.; Sun, R.; Huan, N.; Pan, L. Ground-level ozone in urban Beijing over a 1-year period: Temporal variations and relationship to atmospheric oxidation. *Atmos. Res.* **2015**, *164–165*, 110–117. [[CrossRef](#)]
20. Wang, G.; Zhang, R.; Gomez, M.E.; Yang, L.; Levy Zamora, M.; Hu, M.; Lin, Y.; Peng, J.; Guo, S.; Meng, J.; et al. Persistent sulfate formation from London Fog to Chinese haze. *Proc. Natl. Acad. Sci. USA* **2016**, *113*, 13630–13635. [[CrossRef](#)] [[PubMed](#)]
21. Su, Z.; Wang, J. Pollution characteristics and determinants of atmospheric particulate matter and its determinants in Guiyang. *Acta Sci. Nat. Univ. Sunyatseni* **2015**, *54*, 77–84. (In Chinese)
22. Sillman, S.; Logan, J.A.; Wofsy, S.C. The sensitivity of ozone to nitrogen oxides and hydrocarbons in regional ozone episodes. *J. Geophys. Res. Atmos.* **1990**, *95*, 1837–1851. [[CrossRef](#)]
23. Lu, K.D.; Rohrer, F.; Holland, F.; Fuchs, H.; Bohn, B.; Brauers, T.; Chang, C.C.; Häsel, R.; Hu, M.; Kita, K.; et al. Observation and modelling of OH and HO<sub>2</sub> concentrations in the Pearl River Delta 2006: A missing OH source in a VOC rich atmosphere. *Atmos. Chem. Phys.* **2012**, *12*, 1541–1569. [[CrossRef](#)]
24. Wang, Y.; Yao, L.; Wang, L.; Liu, Z.; Ji, D.; Tang, G.; Zhang, J.; Sun, Y.; Hu, B.; Xin, J. Mechanism for the formation of the January 2013 heavy haze pollution episode over central and eastern China. *Sci. China Earth Sci.* **2013**, *57*, 14–25. [[CrossRef](#)]
25. Gen, M.; Zhang, R.; Huang, D.D.; Li, Y.; Chan, C.K. Heterogeneous SO<sub>2</sub> Oxidation in Sulfate Formation by Photolysis of Particulate Nitrate. *Environ. Sci. Technol. Lett.* **2019**, *6*, 86–91. [[CrossRef](#)]
26. Heintzenberg, J. Fine particles in the global troposphere: A review. *Tellus* **1989**, *B41*, 149–160. [[CrossRef](#)]
27. Sun, W.; Wang, D.; Yao, L.; Fu, H.; Fu, Q.; Wang, H.; Li, Q.; Wang, L.; Yang, X.; Xian, A.; et al. Chemistry-triggered events of PM<sub>2.5</sub> explosive growth during late autumn and winter in Shanghai, China. *Environ. Pollut.* **2019**, *254*, 112864. [[CrossRef](#)] [[PubMed](#)]
28. Wang, G.; Zhang, F.; Peng, J.; Duan, L.; Ji, Y.; Marrero-Ortiz, W.; Wang, J.; Li, J.; Wu, C.; Cao, C.; et al. Particle acidity and sulfate production during severe haze events in China cannot be reliably inferred by assuming a mixture of inorganic salts. *Atmos. Chem. Phys.* **2018**, *18*, 10123–10132. [[CrossRef](#)]
29. Zhang, B.; Wang, Y.; Hao, J. Simulating aerosol–radiation–cloud feedbacks on meteorology and air quality over eastern China under severe haze conditions in winter. *Atmos. Chem. Phys.* **2015**, *15*, 2387–2404. [[CrossRef](#)]